Characterization of two cDNAs encoding auxin-binding proteins in Nicotiana tabacum

Nathalie Leblanc-Fournier, Camille Roux, Jean-Marc Pradier, Catherine Perrot-Rechenmann

Plant Molecular Biology **33:** 679–689, 1997.

Characterization of two cDNAs encoding auxin-binding proteins in *Nicotiana tabacum*

Nathalie Leblanc, Camille Roux, Jean-Marc Pradier and Catherine Perrot-Rechenmann*
*Institut des Sciences végétales, CNRS, Bâtiment 23, Avenue de la Terrasse, F-91198 Gif sur Yvette, France (*author for correspondence)*

Received 26 January 1996; accepted in revised form 18 November 1996

Key words: Auxin-binding proteins, *Nicotiana tabacum*, RT-PCR analysis, organ-specific expression, recombinant Nt-ERabp[1]

Abstract

The isolation and the characterization of two tobacco cDNAs, *Nt-ERabp1* and *Nt-ERabp2*, homologous to *Zm-ERabp1*, encoding the major auxin-binding protein from maize coleoptiles, are described. Their predicted amino acid sequences correspond to proteins of ca. 21 kDa, in which the characteristic regions common to ABP1-related polypeptides are well-conserved. Southern analysis indicates that the genes corresponding to *Nt-ERabp1* cDNA and *Nt-ERabp2* cDNA derive respectively from *Nicotiana tomentosiformis* and *Nicotiana sylvestris*, the diploid progenitors of *Nicotiana tabacum*. Analysis of mRNA distribution in tobacco plants indicates that these two genes are preferentially expressed in flowers and growing seedlings. Whatever the tissue tested, *Nt-ERabp1* mRNA is more abundant than *Nt-ERabp2* mRNA. Furthermore, RT-PCR reveals developmental and organ-specific expression of these two genes in flower parts of tobacco plants. In particular, regulation of *Nt-ERabp1* mRNA accumulation appears to be correlated with elongation growth of each floral organ. Recombinant Nt-ERabp1, produced in *Escherichia coli*, is recognized by antibodies raised against Zm-ERabp1.

Introduction

The plant hormone auxin has been shown to be involved in the regulation of a wide range of responses in the growth and development of plants (for review, see [4]). In an attempt to better understand mechanisms by which the auxin signal is perceived by cells, several laboratories have isolated different auxin-binding proteins (for reviews, see [12, 28]). Among these proteins, the auxin-binding protein Zm-ERabp1 purified from maize coleoptiles [16, 19, 24] is now well characterized. The primary translation product deduced from the isolated cDNAs [9, 11, 27] was calculated to be ca. 22 kDa (201AA). This sequence contained a 38 residue N-terminal signal sequence, which was cleaved to produce the mature protein, and a KDEL tetrapeptide localized at the C-terminal end of the protein, which is known to be a retention signal for proteins in the lumen of the endoplasmic reticulum. Using the electrical membrane response to auxin of tobacco mesophyll protoplasts as a functional assay, Barbier-Brygoo *et al.* [2] have shown that antibodies raised against Zm-ERabp1 were able to inhibit the auxin-induced hyperpolarization of tobacco protoplasts, suggesting that a protein immunologically related to Zm-ERabp1 was involved in auxin perception. The incubation of tobacco protoplasts with exogenous Zm-ERabp1 increased the sensitivity to auxin of the electrical membrane response. Antibodies raised against a synthetic peptide (D16), corresponding to a putative binding site for auxin within the Zm-ERabp1 protein, were shown to have an auxin-agonist activity on this electrical response [29]. These results have been recently reinforced by patch-clamp analysis performed on maize coleoptile protoplasts. These experiments have demonstrated that auxin induced an increase of H^+ current at the plasma membrane, current which is thought to reflect activation of the PM-localized H^+-ATPase. Whereas this H^+ current is abolished with polyclonal anti-Zm-ERabp1, D16 polyclonal antibodies enhanced this current in an

auxin-like manner [21]. Furthermore, voltage-clamp analyses of guard cells of *Vicia faba* have shown that a synthetic peptide corresponding to the C-terminal part of Zm-ERabp1 is able to inactivate the inward K^+ channels of plasma membrane, mimicking in this way the effects of high concentrations of auxin [26]. Finally, even if the biochemical characteristics of Zm-ERabp1 suggested a localization of the protein in the ER, recent experiments performed on maize coleoptile protoplasts have indicated that a fraction of the protein could be detected at the external face of the protoplasts [6]. All these data are in favour of a possible involvement of Zm-ERabp1 in the auxin perception at the plasma membrane level.

Immunologically related ABP1 proteins have been detected in other plant species such as pea, mung bean and barnyard grass [29]. Whereas both genomic sequences and cDNAs, homologous to *Zm-ERabp1*, have been reported for different dicotyledonous plants such as *Arabidopsis* [20] or strawberry [12, 15], the function of the corresponding proteins has been poorly studied. In tobacco plants, D16 antibodies were shown to cross-react with a protein of ca. 22 kDa in partly purified microsomal protein fractions of tobacco leaves [29]. Until now, no molecular tools have been developed from this plant material to further study the auxin electrical response and gain insight into the auxin perception system at the plasma membrane on tobacco.

As a first step towards a better understanding of auxin perception in tobacco plants, we have isolated two cDNAs sharing homology with the *Zm-ERabp1* gene using a RT-PCR procedure. These PCR fragments were used to obtain full-length cDNAs from a tobacco seedling cDNA library. The *ABP1* gene family in the tobacco genome was characterized by Southern blot analysis and we have studied the specific expression of these two genes in various organs of tobacco plants and in floral organs during flower development. The production of recombinant Nt-ERabp1 protein in *E. coli* is also reported.

Materials and methods

Plant material

Tobacco plants (*Nicotiana tabacum* cv. Xanthi, wild-type clone XHFD8 and its progenitor species *Nicotiana sylvestris* and *Nicotiana tomentosiformis*) were grown from seeds in a greenhouse (22 °C, 9 h of light per day or 16 h of light per day for flowering).

Nt-ERabp cDNAs isolation

To synthesize first-strand cDNA, 1 μg poly(A)$^+$ RNA extracted from tobacco leaves and previously treated with DNaseRQ1 (Promega), was incubated in presence of 0.5 μg of oligo(dT)$_{12-18}$ in buffer containing 80 mM Tris-HCl pH 8.3, 30 mM KCl, 6 mM $MgCl_2$, 8 mM DTT, 80 μg/ml BSA (RNase-free), 0.5 mM of each dNTP and 40 U RNasin (Promega). After addition of 200 U of M-ML V reverse transcriptase (Gibco-BRL) and 10 U of AMV reverse transcriptase (Promega), samples were incubated for 90 min at 42 °C. One third of the reaction volume was used to perform the amplification procedure. To amplify the two *Nt-ERabp* cDNAs, 3 oligonucleotides were synthesized. The 25-mer primers 85A (5′-TCGCCATGTTCTCGTAGTGGTAGCT-3′) and 92A (5′-CCCGCCACATCATCATACTAGTTGC-3′) correspond specifically to the 5′ end of the ORF of each *Nt-ERabp* cDNA, as predicted by sequence analysis of genomic clones *Ntt85A* and *Ntt92A* registered in the gene bank [25]. The third primer END (5′-GCTCATCTTTCCACGAAGTTGTCTG-3′) which matches the 3′ end of the ORF of *Ntt85A* and differs only in one nucleotide in *Ntt92A*, was used as antisense primer in the two reactions. Amplification procedure was performed with 1 U of Taq polymerase (Promega) in the presence of 2 μM of the primers and 200 μM of each dNTP. PCR conditions were 94 °C for 3 min, followed by 30 cycles (94 °C for 30 s, 65 °C for 2 min, 72 °C for 2 min), and finished by 5 min at 72 °C. The PCR fragments were subcloned into pBlueScript vector and sequenced using T7DNAPol sequencing kit (Pharmacia).

To obtain full-length cDNAs, an auxin-induced tobacco seedling cDNA library constructed in the laboratory (Dargeviciute, unpublished results) using the Stratagene Zap-cDNA GigapackII gold cloning kit was screened with one of the RT-PCR fragment probe. Hybridization was done at 65 °C in the hybridization buffer (HB) containing 4× SSC, 10× Denhardt's solution, 20 mM sodium phosphate buffer pH 7, 7% SDS, and 100 μg/ml salmon sperm DNA. Three positive clones were selected from 800 000 recombinant plaques obtained from one-time amplified λZap library. After further purification through 3 successive rounds of screening, the λZap clones were excised *in vivo* following the manufacturer's instructions (Stratagene). Clones were then sequenced by using the Pharmacia kit.

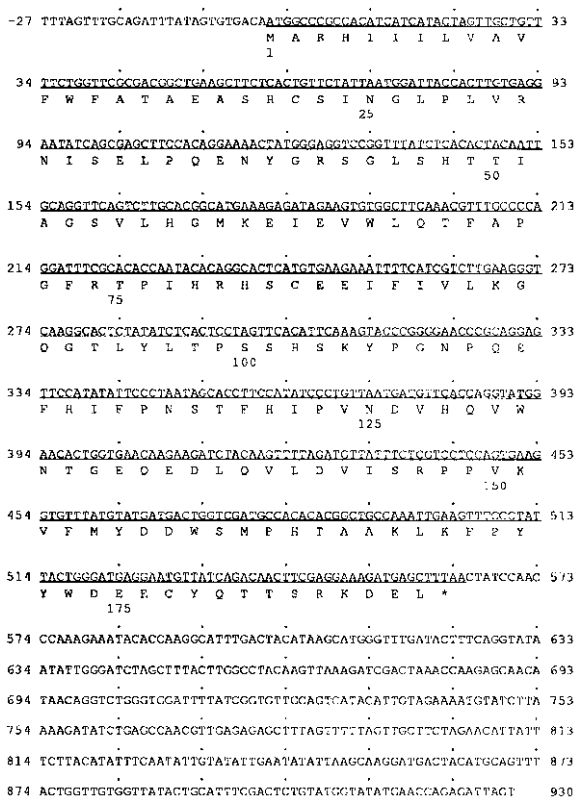

Figure 1. Nucleotide sequence of *Nt-ERabp2* cDNA and its deduced amino acid sequence.

Southern blot analysis

Plant DNA was purified from leaves of different tobacco plant species as described by [5]. Genomic DNA (5 μg) was digested to completion with the restriction enzymes indicated in Fig. 4. DNA fragments were analyzed by electrophoresis in 0.6% Seakem agarose gel (FMC) at 40 V for 16 h in 1× TBE. After HCl treatment, the gel was capillary blotted onto Hybond-N^+ membrane in alkaline conditions (0.5 M NaOH). Membrane was hybridized with $\alpha - [^{32}P]$-dCTP-labelled *Nt-ERabp1* PCR fragment at 60 °C in buffer HB. Filter was then washed in low-stringency conditions (1× SSC, 0.1% SDS) at 60 °C.

Northern blot analysis

Total RNA was prepared from tobacco plant tissues as described [17]. Poly(A)$^+$ RNA were selected by chromatography on oligo(dT) cellulose (Pharmacia) according to the standard method [1]. 4 μg of poly(A)$^+$ RNA was electrophoresed through 1% agarose gels containing 50% formaldehyde [22]. The gel was capillary blotted onto Hybond-N membrane (Amersham) in 10× SSC. RNA was subsequently UV cross-linked to the membrane. To increase the radioactive signal, *Nt-ERabp1* PCR fragments were labelled using both α-[^{32}P]-dCTP and α-[^{32}P]-dATP by the random priming Megaprime. Kit (Amersham). Hybridization was performed at 65 °C in buffer HB. The membrane was then washed at 65 °C in high-stringency conditions up to 0.5× SSC, 0.1% SDS, and exposed to a film between intensifying sheets for times varying between 5 days and 2 weeks or quantified using a phosphor-imager equipment (Molecular Dynamics).

RT-PCR analysis

To visualize the differential expression of the two *Nt-ERabp* genes, first-strand cDNA was synthesized from 0.5 μg of poly(A)$^+$ RNA purified from the different plant tissues as previously described. One fourth of each cDNA sample was amplified either with the pair of primers 85A-END to specifically amplify the *Nt-ERabp1* cDNA, or with the pair 92A-END for *Nt-ERabp2*. After a first cycle with heating denaturation for 3 min at 94 °C, a PCR of 20 cycles (94 °C, 1 min; 68 °C, 2 min; 70 °C, 2 min) was performed. This number of cycles was determined so as to stay in the exponential phase of PCR. PCR products were subjected to electrophoresis on 1% agarose gel (Appligene) and blotted onto Hybond-N^+ membrane (Amersham) in alkaline conditions. Membranes were hybridized in standard conditions at 65 °C with $\alpha - [^{32}P]$-dCTP-labelled *Nt-ERabp1* probe obtained using the random priming Megaprime kit (Amersham). In the case of experiments shown in Fig. 5C, a PCR of 30 cycles was performed to allow the visualization of *Nt-ERabp2* expression in all organs tested. These conditions are no longer quantitative for *Nt-ERabp1* transcripts which are more abundant.

Expression of Nt-ERabp1 in Escherichia coli

The expression of recombinant Nt-ERabp1 in *E. coli* was performed by using the pQE30 expression vector which contains an affinity tag consisting of 6 consecutive histidine residues (6×His tag) (Qiaexpress expression system, Qiagen). One *BamH1* restriction site was added at each end of the sequence *Nt-ERabp1*, and the ATG codon was deleted to use the initiator codon included in the vector. These modifications were introduced by amplification of

the *Nt-ERabp1* fragment with the two primers 5′-ATACGGATCCGCTCGCCATGTTCTCGTAGTGGT AG-3′ for the amino terminal side, and 5′-CGCGGATCCTTAAAGCTCATCTTTCCACGAAGT TGT-3′ for the carboxyl terminal side. PCR conditions were 94 °C for 3 min, followed by 25 cycles (94 °C for 30 s, 65 °C for 2 min, 72 °C for 2 min). After sequencing of these PCR fragments sub-cloned in pBS vector with T7DNAPol kit (Pharmacia), these sequences were inserted in the *Bam*HI cloning site of pQE30, located downstream the 6×His affinity tag. *E. coli* cells (M15) transformed with the recombinant plasmid pQE30-*Nt-ERabp1* were grown to 0.7 O.D. Cells were harvested 3 h after induction with 2 mM IPTG and collected by centrifugation at 1000 × *g* for 10 min. The pellet was resuspended in sonication buffer (50 mM sodium phosphate pH 7.8, 300 mM NaCl, 5 mM EDTA, 2 mM DTT), subjected to one cycle of freeze-thaw, sonicated and centrifuged at 10 000 × *g* for 20 min. The supernatant containing soluble proteins was kept at −20 °C with 10% glycerol until further analysis. The pellet was resuspended in the sonication buffer and vortexed for 30 min in the presence of DNaseI (10 μg/ml). Samples were submitted to SDS-PAGE on a 12.5% acrylamide gel [13]. After staining with a cold solution containing 250 mM KCl and 1 mM DTT, the band of correct size was cut out, and grounded with a Potter in PBS (120 mM NaCl, 2.7 mM KCl, 10 mM phosphate buffer pH 7.4). Acrylamide was pelleted by centrifugation at 18 000 × *g* for 20 min. The supernatant was concentrated by filtration on Centricon-3 concentrators (Amicon). Proteins contained in the concentrate were analysed by western blotting and stored at −20 °C with 10% glycerol until further use.

Results

Isolation of two Nt-ERabp *cDNAs*

The primary objective of this work was to clone full-length tobacco cDNAs encoding ABP1-like proteins in tobacco plants. After analysis of the maize and *Arabidopsis ABP1* sequences [9, 20], oligonucleotides corresponding to well conserved domains (boxes A and B) were first used to isolate partial cDNA sequences (data not shown). Then, as two tobacco genomic clones (*Ntt85* and *Ntt92*), showing high homology with *Zm-ERabp* genes, were registered in GenBank database [25], we designed 3 specific oligonucleotides (85A, 92A, END) allowing to isolate longer cDNA fragments. The two primer pairs (85A-END) and (92A-END) were used in a reverse transcription polymerase chain reaction procedure (RT-PCR) to amplify specific cDNAs, synthesized from tobacco leaf poly(A)$^+$ RNA. A single PCR product of 564 bp was obtained for each primer pair. Sequence analysis of these clones demonstrated that *Nt-ERabp1*, the fragment amplified with 85A-END primers, corresponded exactly to the predicted sequence of the open reading frame of *Ntt85a* genomic clone, whereas *Nt-ERabp2* matches that of the *Ntt92a* genomic clone. This result reveals that the two *Ntt85* and *Ntt92* genes are effectively expressed in tobacco leaf tissues.

Sequence analysis of Nt-ERabp2 cDNA

To isolate full-length clones, the PCR fragment corresponding to *Nt-ERabp1* was used as hybridization probe to screen a λZap cDNA library constructed from IAA-induced tobacco seedling mRNAs. Among 800 000 recombinant plaques obtained from the amplified cDNA library, only 3 positive clones were detected. After *in vivo* excision, sequence analysis of each clone demonstrated that two of these clones corresponded to a partial fragment of *Nt-ERabp1* sequence. The third one corresponded to the full-length cDNA of *Nt-ERabp2* sequence.

The complete nucleotide sequence of the cloned cDNA *Nt-ERabp2* and its deduced amino acid sequence are shown in Fig. 1. The cDNA is 957 bp long and contains an open reading frame of 564 bp. A short 5′ non coding region of 27 bp precedes the ATG initiation codon. Surrounding the ATG codon, the conserved motif ACAATGGCC is consistent with the initiator consensus sequences described for plant [16]. The long 3"-untranslated region of 366 bp contains a potential polyadenylation site at position 844 but no poly(A) tail has been detected. The absence of the extensive 3′-terminal poly(A) results probably from cloning artefacts since first-strand cDNA was synthetized using an oligo(dT)$_{12-18}$ primer.

The primary protein of Nt-ERabp2 was calculated to be 21.4 kDa (187AA). A putative site for signal peptidase activity is located between the Ala-19 and Ser-20 residues of the amino acid sequence. The deduced mature protein would then be 19.3 kDa (pI 6.3).

Comparison of amino acid sequences of Nt-ERabp1 and Nt-ERabp2 presented in Fig. 2 shows clearly a high degree of homology between these two proteins. The predicted amino acid sequence of Nt-ERabp1 also encodes a mature protein of 19 kDa

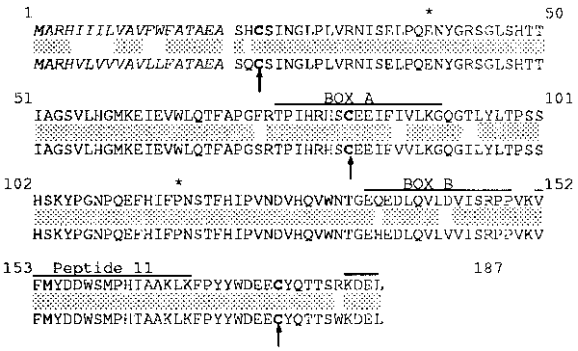

Figure 2. Comparison of the amino acid sequences of Nt-ERabp2 (upper lane) and Nt-ERabp1 (bottom lane). The two potential N-glycosylation sites are shown by an asterisk. The underlined regions correspond to highly-conserved domains of ABP1-like proteins: Box A and peptide 11 are two regions described in maize to be potentially involved in auxin binding [29, 3], no function has yet been assigned to Box B. Arrows indicate conserved cysteine residues in ABP1-like proteins.

(pI 6.3). Only 7 amino acids differ from one protein to the other, 5 of them corresponding to conservative substitutions. These results are in accordance with the high degree of homology (95%) observed at the nucleic acid level between these two cDNAs.

The particular regions typifying ABP1 proteins are very well conserved in the tobacco proteins: the 3 cysteine residues (C-22, C-82, C-177), the C-terminal KDEL tetrapeptide, box A and peptide 11 regions potentially involved in auxin binding [29, 3] and the box B region for which no function has yet been assigned (see Fig. 2). In common with ABP1 sequence from *Arabidopsis*, two potential N-glycosylation sites are present at position N-40 and N-132 within the tobacco sequences. These two potential N-glycosylation sites were also described in the *Arabidopsis* and strawberry sequences (the latter sequence showing an additional site) while only one site was observed in the maize sequences. All of these data indicate that the two *Nt-ERabp* sequences encode proteins homologous to Zm-ERabp1.

Southern blot analysis

To better characterize the *Nt-ERabp* gene family in *N. tabacum*, genomic DNA was digested with *Bam*HI, *Hin*dIII and *Eco*RI and probed under low stringency conditions with a fragment corresponding to the entire ORF of *Nt-ERabp*1. In the *Bam*HI restriction lane of *N. tabacum* genome, three fragments are detected: two bands of high molecular weight (>7 kb) and one band

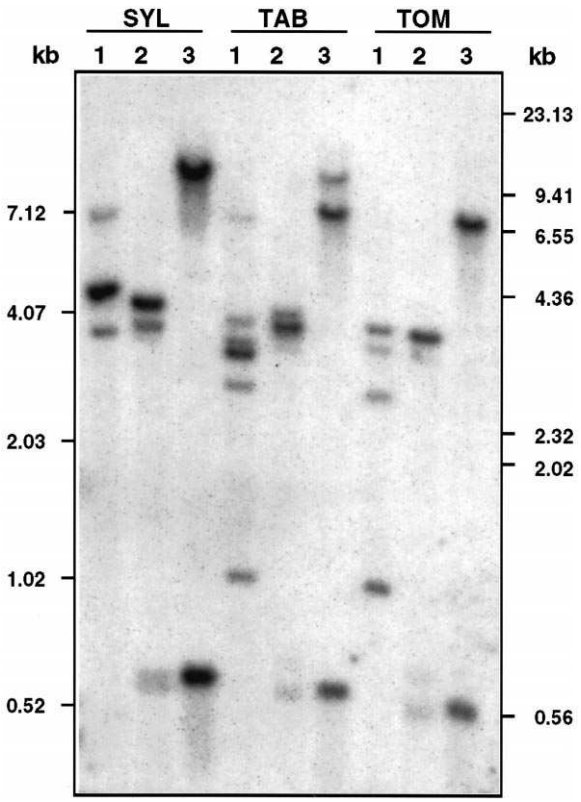

Figure 3. Southern analysis of tobacco genomic DNA. Total genomic DNA was isolated from leaves of *N. sylvestris* (SYL), *N. tabacum* (TAB) and *N. tomentosiformis* (TOM) and digested with *Eco*RI (lane 1), *Hin*dIII (lane 2) and *Bam*HI (lane 3). The resulting digests were separated on 0.6% agarose gel, transferred to a nylon membrane and probed with a [^{32}P]-labelled fragment corresponding to *Nt-ERabp1* under low-stringency conditions. Each lane contained 5 μg DNA. The molecular weight markers *Hin*dIII digested phage λ and 1 kb ladder (Gibco) are shown in kb at the right and left respectively.

of ca. 600 bp (Fig. 3). However, when total genomic DNA was amplified with oligonucleotide couples (85A-END) and (92A-END), the 3 kb PCR fragments, corresponding to the region localized between exon 1 and exon 5 of each gene, were not digested by *Bam*H1 restriction enzyme (data not shown). These results suggested that the two fragments larger than 7 kb corresponded to the *Ntt85A* and *Ntt92A* genes previously described. The fragment of about 600 bp demonstrated the presence of a third genomic sequence sharing homology with *Nt-ERabp* genes.

Comparison of the two cDNAs *Nt-ERabp1* and *Nt-ERabp2* showed 95% homology at the nucleic acid level. As the *N. tabacum* genome is amphidiploid, it was of particular interest to determine whether these two genes are present or not in its diploid progenit-

ors *N. tomentosiformis* and *N. sylvestris*. Among the two bands of high molecular weight observed after *Bam*HI digestion of *N. tabacum* genomic DNA, the upper one is observed in *N. sylvestris* and the lower one in *N. tomentosiformis*. Digestion of genomic clones *Ntt85A* and *Ntt92A* with *Eco*RI was expected to give three restriction fragments in the case of *Ntt85A* gene, including one band of 1100 bp, whereas only two bands of unknown molecular size were expected for *Ntt92A*. Southern blot analysis showed clearly that the 1100 bp band is detected in *N. tomentosiformis* and in *N. tabacum*, but not in *N. sylvestris* (Fig. 3). These data indicated that *Ntt85A* gene derived from *N. tomentosiformis* genome and *Ntt92A* gene from *N. sylvestris*. Therefore, the genes *Ntt85A* and *Ntt92A* correspond to homeogenes, and encode proteins of similar function. PCR data using 85A-END and 92A-END specific primers for the amplification of genomic DNA from the three tobacco species also reinforced this analysis (data not shown). Whereas all bands detected in *N. tomentosiformis* are present in *N. tabacum*, some fragments present in *Eco*RI and *Hin*dIII restriction patterns of *N. sylvestris* are not observed in *N. tabacum* ones. Therefore, we cannot exclude that some modifications have occurred after the crossing between the two species.

The 600 bp fragment observed in *Bam*HI restriction pattern of *N. tabacum* is present in both *N. tomentosiformis* and *N. sylvestris*.

Organ-specific expression of tobacco Nt-ERabp *genes*

To perform RNA blot analysis, the PCR fragment corresponding to the coding sequence of *Nt-ERabp1* was used as probe, with hybridization and washing conditions that did not allow us to distinguish between the two different *Nt-ERabp* transcripts. As shown in Fig. 4A, only one transcript of ca. 1 kb is detected in mRNA isolated from young tobacco seedlings, treated or not by using 10 μM of NAA. In both conditions, the level of *Nt-ERabp* mRNA is identical.

To study the distribution of *Nt-ERabp* mRNAs in various organs of tobacco plants, poly(A)$^+$ RNA isolated from seedlings, flowers, flower buds, young leaves, stems, and young roots were subjected to RNA gel blot analysis. Whatever the organ tested, no signal could be detected on total RNA, and even using poly(A)$^+$ RNA, a long exposure time was required to detect a signal. This result reveals low expression levels of these genes in tobacco plants, in agreement with the low number of cDNA clones isolated from the

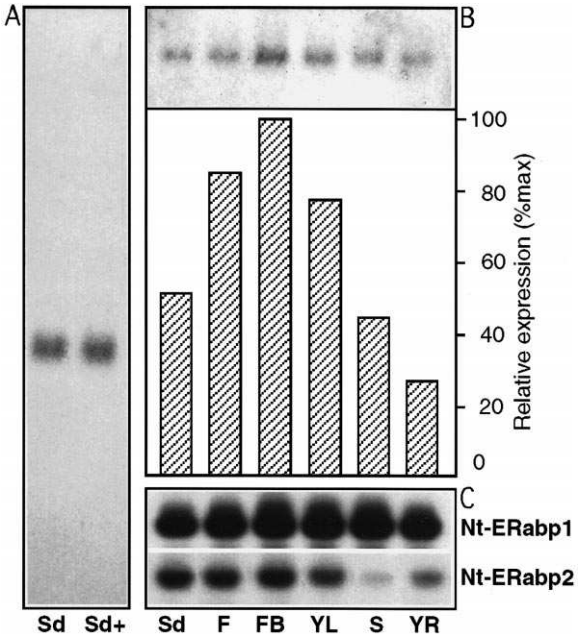

Figure 4. Tissue-specific expression of *Nt-ERabp1* and *Nt-ERabp2* in *N. tabacum* plants. A. Northern blot of poly(A)$^+$ RNA (4 μg per lane) extracted from tobacco seedlings grown in liquid medium treated (Sd+) or not (Sd) with 10 μM NAA for 2 h. The filter was probed with [^{32}P]-labelled *Nt-ERabp1*. B. Histogram showing differences in *Nt-ERabp* mRNA accumulation in tobacco seedlings (Sd), flower buds (FB), flowers (F), young leaves (YL), stems (S) and young roots (YR). The filter was probed with [^{32}P]-labelled *Nt-ERabp1*. The hybridization signals were quantified by a Bioimage analyser system (Millipore). C. Specific expression of each *Nt-ERabp* gene determined by RT-PCR experiments. The oligonucleotide pairs (85A-END) and (92A-END) were used to amplify specifically *Nt-ERabp1* and *Nt-ERabp2* cDNAs, respectively. A PCR of 30 cycles was performed with cDNA samples synthesized from 0.5 μg mRNA of each tobacco organs (Sd, FB, F, YL, S, YR). PCR fragments were separated on agarose gels, transferred onto nylon membrane and hybridized with [^{32}P]-labelled *Nt-ERabp1*.

cDNA library. As shown in Fig. 4B, the transcripts are detected in all organs tested. *Nt-ERabp* genes are predominantly expressed in developing flowers and young leaves while lower amounts are detected in young roots. The relative amount of these transcripts is significantly reduced in developed organs as the leaves and the roots (data not shown).

To study the specific expression of each *Nt-ERabp* gene in the same samples and according to the low expression level of these genes in tobacco plants, RT-PCR analysis was also performed (Fig. 4C). This study was carried out by using the two oligonucleotide pairs (85A-END) and (92A-END) to amplify specifically the corresponding cDNAs obtained from mRNAs of the different organs. After blotting of the

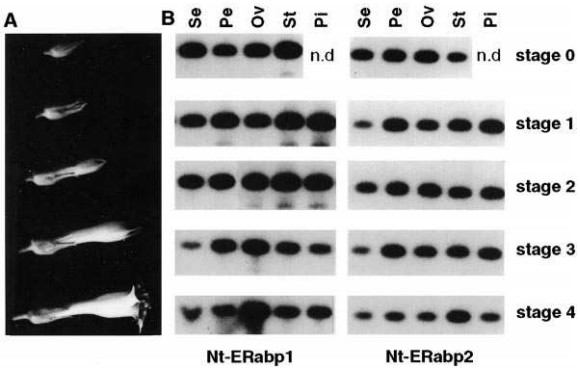

Figure 5. Specific expression of *Nt-ERabp* genes in flower parts during flower development. A. Photographs of flowers at the different stages (F_0 to F_4) of development defined to perform the expression analysis. B. Expression of *Nt-ERabp* genes in flower parts studied by RT-PCR. The oligonucleotide pairs (85A-END) and (92A-END) were used to amplify specifically *Nt-ERabp1* cDNA and *Nt-ERabp2* cDNA respectively. First-strand cDNAs were synthesized from 0.5 μg mRNA of stamens (St), pistils (Pi), ovaries (Ov), petals (Pe) and sepals (Se) of flowers at the different stages of flower development described in (A). 20 cycles of PCR were performed to be under semi-quantitative conditions. n.d., not determined.

PCR products onto nylon membrane, the blots were hybridized with a radiolabelled *Nt-ERabp1* probe. As a control, PCR fragments were digested in parallel with *Bsm*I, a restriction enzyme specific to the *Nt-ERabp1* cDNA sequence. Results have indicated that in our conditions, each oligonucleotide pair is specific to the corresponding *Nt-ERabp* (data not shown). In all organs tested, *Nt-ERabp1* transcripts are much more abundant than *Nt-ERabp2*. Thus, to visualize the expression of *Nt-ERabp2* in all organs tested, a PCR of 30 cycles was performed (Fig. 5C). Under these conditions, PCR products corresponding to *Nt-ERabp1* accumulated in a non-quantitative manner due to the higher abundance of this transcript. This means that direct comparison between these results and northern blot analysis is not relevant. However, these data suggested that hybridizing signals observed with northern blot analysis corresponded mainly to *Nt-ERabp1* transcripts. This analysis demonstrates that both genes are predominantly expressed in flowers buds. Slight differences in the expression patterns could be detected between the two genes. For instance, *Nt-ERabp1* is also well expressed in stems whereas *Nt-ERabp2* mRNA is relatively more abundant in young roots than in stems.

Nt-ERabp-*specific expression in developing flowers*

We have further studied the distribution of *Nt-ERabp* transcripts in flowers by determining the level of both messengers in floral organs at different stages of development (Fig. 5A). At stage O, all floral organs are already differentiated and then are essentially subjected to cell elongation until stage 4 when the flower opens.

To distinguish the two *Nt-ERabp* transcripts, this analysis was carried out with a RT-PCR procedure under semi-quantitative conditions for both transcripts (20 cycles). As shown in Fig. 5B, differences are observed between the expression patterns of the two genes. For instance, whereas the steady-state level of *Nt-ERabp2* mRNA is constant during stamen development, the *Nt-ERabp1* mRNA level decreases from stage 0 to stage 4. The same cDNA samples were used for the amplification reactions of the two fragments. These experiments were performed several times from two independent syntheses of cDNAs. In addition, we have confirmed that the two couples of primers amplified the corresponding Nt-ERabp sequence with the same efficiency (data not shown). Therefore, the variations observed for one gene in comparison with the other reflected significant differential expression in the various floral parts. *Nt-ERabp1* appeared to be more highly expressed than *Nt-ERabp2* in all samples.

To better analyse the regulation of the expression during flower development, hybridization signals were quantified for each organ as a function of flower development stage. As shown in Fig. 6, high expression levels of *Nt-ERabp1* were observed in pistils and stamens of flower buds. The levels decreased slowly until stage 4 where 3–4-fold less mRNA was detected. *Nt-ERabp1* mRNA accumulated continuously from stage 0 to stage 4 in ovaries which can be correlated with the unceasing growth of this organ along fruit development. As shown in Fig. 6A, sepal development seems to be already completed at first stage. Interestingly, sepals are the organs where the levels of *Nt-ERabp1* are the lowest from stage 2 of flower development (Fig. 6). In petals, *Nt-ERabp1* mRNA accumulates and reaches a maximum at stage 2, where the petals are subjected to rapid elongation (Fig. 6A). The mRNA level then rapidly decreases between stage 2 and stage 4 when the flower opens. These differences of *Nt-ERabp1* mRNA accumulation were not observed for *Nt-ERabp2* which showed less variation during flower development.

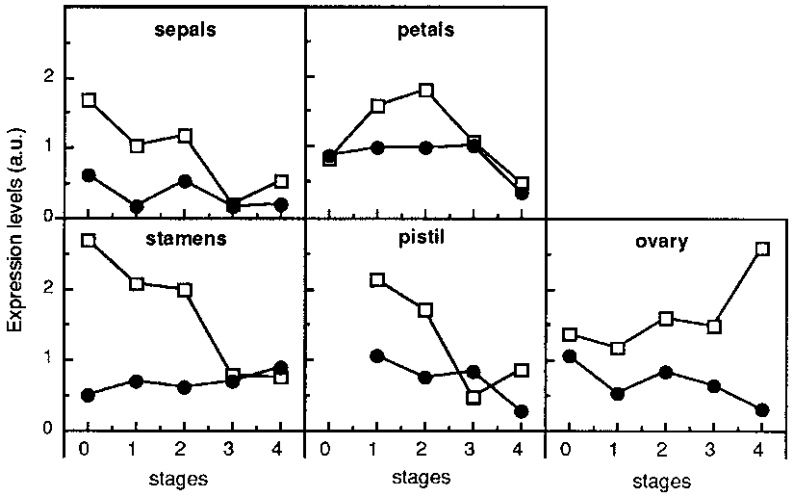

Figure 6. Curves showing for each flower organ the level of *Nt-ERabp*1 (-□-) and *Nt-ERabp2* (-●-) transcripts as a function of developmental stage. The mRNA levels (arbitrary units) were determined by quantification of the hybridization signals shown in Fig. 5B using a Bioimage analyser system (Millipore).

Expression of Nt-ERabp1 *in* E. coli

The low abundance of ABP1-related proteins in tobacco did not allowed their purification from plant material. Therefore, the Nt-ERabp1 protein was produced in *E. coli* using the 6×His tag pQE-30 expression vector. As shown on the silver-staining profile in Fig. 7, one polypeptide of ca. 22.5 kDa is accumulated in inclusion bodies after 3 h of IPTG induction. This protein represents about 40% of the total proteins contained in insoluble fractions. Western blot analysis showed that two polypeptides of 21 kDa and 22.5 kDa share immunological homology with Zm-ERabp1 since they are recognized by polyclonal antibodies raised against this protein (Fig. 7). These two polypeptides are also recognized by D16, a polyclonal antibody raised against a synthetic peptide corresponding to a putative auxin-binding site of Zm-ERabp1 [29]. The 22.5 kDa form corresponds to the expected size, by adding the 6×His tag (900 Da) to the molecular mass predicted by the amino acid sequence of Nt-ERabp1 (21.3 kDa).

The molecular mass of the 21 kDa polypeptide is lower than predicted. The monoclonal antibody 2E7, directed against a synthetic peptide HDEL (His-Asp-Glu-Lys) recognized specifically the two polypeptides. According to these results, the 21 kDa form, which contains the C-terminus KDEL tetrapeptide, corresponds probably to a partial Nt-ERabp1 which could have lost part of the N-terminus region of the protein, including the 6×His tag. Analysis of the enriched product (P) using SDS-PAGE showed that one major band of 22.5 kDa is detected after silver staining, and cross-reacts with both the anti-Zm-ERabp1 polyclonal antibodies and the anti-HDEL monoclonal antibody (Fig. 7). Such procedure has allowed the production of 20 mg of purified Nt-ERabp1 per litre of bacterial culture.

Discussion

Among the various auxin-binding proteins already identified, the maize ABP1 was proposed to be involved in the auxin perception at the plasma membrane. In particular, experimental evidence has been provided by the study of the electrical membrane response to auxin of tobacco mesophyll protoplasts [2]. To go further in the characterization of the auxin perception system involved in this early auxin response, we have developed molecular tools on tobacco.

In this paper, we describe the molecular cloning of two cDNAs from tobacco plants, *Nt-ERabp1* and *Nt-ERabp2*, thus demonstrating the expression of the two genes *Ntt85A* and *NTT92A* previously introduced in Gene data bank [25]. The encoded proteins share 62% homology with the maize protein Zm-ERabp1. The characteristic regions of ABP1-like proteins (Fig. 2) such as the box A and peptide 11 regions supposed to be involved in auxin binding, the box B and the KDEL

tetrapeptide are all present in the amino acid sequences of both tobacco proteins.

The two mature proteins Nt-ERabp1 and Nt-ERabp2 have calculated sizes of 19 kDa and 19.3 kDa respectively. Taking the two potential N-glycosylation sites into account, this molecular mass fits well with the tobacco protein of 22 kDa which cross-react with polyclonal anti-Zm-ERabp1 and with D16 polyclonal antibodies raised to a synthetic peptide corresponding to box A of the maize protein [29].

Southern blot analysis indicated clearly that the two genomic sequences *Ntt85A* and *Ntt92A* identified in the *N. tabacum* genome derived from its ancestral diploid progenitors *N. tomentosiformis* and *N. sylvestris*, respectively. Therefore, we suggest that these two genes correspond to homeogenes, encoding proteins of similar function. These results are in accordance with the high degree of homology (95%) observed between the two cDNAs and their predicted amino acid sequences. In *Arabidopsis* also, only one *Abp1*-related gene was isolated [20]. In maize, at least four genomic sequences have already been identified [9, 10, 23]. The *Zn-ERabp1* and *Zm-ERabp4* genes exhibit differential organ-specific expression and the two genes *Zm-ERabp4* and *Zm-ERabp5*, which share 95% identity, have similar pattern of expression and differ only in their expression levels.

As observed in the *Bam*H1 restriction patterns, a third genomic sequence visualized in the three tobacco species shares homology with *Nt-ERabp* genes. In northern-blot analysis, only one transcript of ca. 1 kb was detected under standard hybridization conditions. At this time, we could not determine whether this third sequence corresponds to a pseudogene related to the *ABP1* family or to another sequence sharing homology with *Nt-ERabp* sequences.

Analysis of *Nt-ERabp* gene expression in floral organs during floral development is well informative about their regulation. First *Nt-ERabp1* was shown to be more expressed than *Nt-ERabp2* and the two genes exhibit differential regulation during floral development. As it is well described in Drews *et al.* [7], even if steps of flower development are identical in the three species. *N. tomentosiformis*, *N. sylvestris* and *N. tabacum*, the flower sizes of these three plants are clearly different. Therefore, we could consider that regulation of the two homeogenes has diverged in the two ancestral species before crossing them to obtain *N. tabacum* plants. However, the shape and pigmentation of *N. tabacum* corolla more closely resemble to *N. tomentosiformis* corolla, whereas the size of corolla

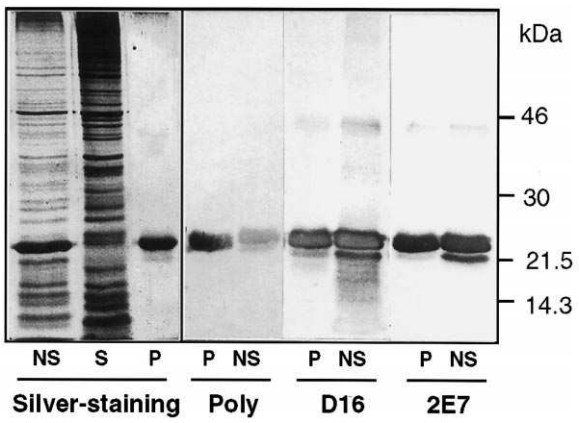

Figure 7. Analysis of recombinant Nt-ERabp1 protein produced in *E. coli*, *E. coli* produced Nt-ERabp1 was analysed by both silver staining and western blot after electrophoresis on SDS-polyacrylamide gel. The lanes contain 2 μg of crude soluble (S) and insoluble (NS) protein fractions or 100 ng of purified Nt-ERabp1 (P) extracted from *E. coli* cells. The western blot procedure was performed by using polyclonal anti-Zm-ERabp1 antibodies (Poly), D16 polyclonal antibodies directed against a synthetic peptide corresponding to BoxA of Zm-ERabp1 protein (D16), or a monoclonal antibody to the HDEL peptide (2E7). Molecular-weight markers are indicated on the right in kDa.

is intermediate between the two progenitors species. With these observations, Drews *et al.* [7] proposed that genes controlling *N. tomentosiformis* corolla pigmentation pattern and shape are dominant to those specifying these characteristics in *N. sylvestris*. Interestingly, the *Nt-ERabp1* gene, which arose from *N. tomentosiformis*, is more highly expressed in all tobacco organs tested and is submitted to regulation during flower development. Further experiments such as the study of expression levels of these genes in ancestral species, would permit determination of whether *Nt-ERabp2* expression is somehow selectively repressed in the *N. tabacum* genome in comparison to *Nt-ERabp1*.

It has been previously suggested that flowers are sites of auxin production in plants and auxin has been shown to influence development of flower parts and fruit setting [14]. In particular, it seems that, in several plants, anthers are one of the sources of auxin in the young flower buds since their removal reduces or completely stops the growth of the bud [14]. Sepals are the first organs to develop and elongate fully, followed by petals, stamens, and pistils. The enlargement of ovaries which continues after fertilization is essentially due to cell expansion. Interestingly, the expression of *Nt-ERabp1* appeared to be regulated during floral development. For instance, higher expression

levels are observed in stamens, stigmas, petals and sepals at the first stages of flower development than in mature flowers when the auxin-requiring growth phase of these flower parts is expected to have been completed. In addition, mRNA accumulation increases continuously in the ovary during its development. In mature flowers, the *Nt-ERabp1* gene is essentially expressed in this organ. These data reinforce the hypothesis of an important role of ABP1-like proteins in flower development.

In maize, *Zm-ERabp1* was shown to be predominantly expressed in coleoptiles, elongating stems and flowers, especially in ears and styles, whereas *Zm-ERabp4* mRNA are more abundant in tassels [9, 10]. More recently, the highest levels of Zm-ERabp1 protein were detected in the apical mesocotyl and basal coleoptile regions, areas which are subject to rapid cell elongation in the etiolated maize seedlings [8]. Several groups have suggested that ABP1-like polypeptides could be involved in a regulatory pathway of auxin-induced cell elongation [12]. Until now, no information was available in dicotyledonous plants and it is of particular interest to observe that in tobacco plants, *Nt-ERabp* messengers accumulate preferentially in tissues able to respond to the hormonal stimulus such as the developing flowers and the young growing organs.

In conclusion, the analysis of *Nt-ERabp* gene expression suggests an interesting correlation between cell elongation process and the *Nt-ERabp1* mRNA accumulation in tobacco. To gain insight into the role of Nt-ERabp1, the study of the protein is required. With this objective, we have first produced Nt-ERabp1 in *E. coli* to obtain significant amounts of unglycosylated recombinant protein which will allow us to raise monoclonal antibodies to peptidic domains of the tobacco protein. Such antibodies will be used to further characterize the protein and to study its possible involvement in the auxin perception system by working in homologous conditions.

Acknowledgements

We thank Ausra Dargeviciute for supplying the cDNAs library, Austra Dargeviciute and Dr Jurg Bilang for assistance in flower dissection, and Dr Beate Knauth and Professor Jean Guern for critical reading of the manuscript.

References

1. Aviv H, Leder P: Purification of biologically active globin messager RNA by chromatography on oligothymidylic acid-cellulose. Proc Natl Acad Sci USA 69: 1408–1412 (1972).
2. Barbier-Brygoo H, Ephritikhine G, Klämbt D, Maurel C, Palme K: Perception of the auxin signal at the plasma membrane of tobacco mesophyll protoplasts. Plant J 1: 83–93 (1991).
3. Brown JC, Jones AM: Mapping the auxin-binding site of auxin-binding protein 1. J Biol Chem 269: 21136–21140 (1994).
4. Davies PJ: Plant hormone and their role in plant growth and development. Martinus Nijhoff/Kluwer Academic Publishers, Dordrecht (1987).
5. Dellaporta SL, Wood J, Hicks JB: A plant DNA minipreparation: Version II. Plant Mol Biol Rep 1: 19–21 (1983).
6. Diekmann V, Venis MA, Robinson DG: Auxins induce clustering of the auxin-binding protein at the surface of maize coleoptiles protoplasts. Proc Natl Acad Sci USA 92: 3425–3429 (1995).
7. Drews GN, Beals TP, Bui AQ, Goldberg RB: Regional and cell-specific gene expression patterns during petal development. Plant Cell 4: 1383–1404 (1992).
8. Harnden D, Jones AM: Organ distribution of auxin-binding protein 1 in the etiolated maize seedling. J Plant Growth Regul 14: 109–113 (1995).
9. Hesse T, Feldwisch J, Balshusemann D, Bauw G, Puype M, Vandekerckhove J, Löbler M, Klämbt D, Schell J, Palme K: Molecular cloning and structural analysis of a gene from *Zea mays* (L.) coding for a putative receptor for the plant hormone auxin. EMBO J 8: 2453–2461 (1989).
10. Hesse T, Garbers C, Brzobohaty B, Kreimer G, Söll D, Melkonian M, Schell J, Palme K: Two members of the ER *abp* gene family are expressed differently in reproductive organs but to similar levels in the coleoptile of maize. Plant Mol Biol 23: 57–66 (1993).
11. Inohara N, Shimomura S, Fukui T, Futai M: Auxin-binding protein located in the endoplasmic reticulum of maize shoots: molecular cloning and complete primary structure. Proc Natl Acad Sci USA 86: 3564–3568 (1989).
12. Jones AM: Auxin-binding proteins. Annu Rev Plant Physiol Plant Mol Biol 45: 393–420 (1994).
13. Laemmli UK: Cleavage of structural proteins during the assembly of the head of bacteriophage T4. Nature 227: 680–685 (1970).
14. Lang: Auxins in flowering. Encycl Plant Physiol 14: 909–950 (1961).
15. Lazarus CM, Macdonald H: Characterization of a strawberry gene for auxin-binding protein, and its expression in insect cells. Plant Mol Biol 31: 267–277 (1996).
16. Löbler M, Klämbt D: Auxin-binding protein from coleoptile membranes of corn (*Zea mays* L.). I. Purification by immunological methods and characterization. J Biol Chem 260: 9848–9853 (1985).
17. Lütcke HA, Chow KC, Mickel FS, Moss HF, Kern HF, Scheele GA: Selection of AUG initiation codons differs in plants and animals. EMBO J 6: 43–48 (1987).
18. Maurel C, Leblanc N, Barbier-Brygoo H, Perrot-Rechenmann C, Bouvier-Durand M, Guern J: Alterations of auxin perception in *rolB*-transformed tobacco protoplasts: Time course of *rolB* mRNA expression and increase in auxin sensitivity reveal multiple control by auxin. Plant Physiol 105: 1209–1215 (1994).

19. Napier RM, Venis MA, Bolton MA, Richardson LI, Butcher GW: Preparation and characterization of monoclonal and polyclonal antibodies to maize membrane auxin-binding proteins. Planta 176: 519–526 (1988).
20. Palme K, Hesse T, Campos N, Garbers C, Yanofsky MF, Schell J: Molecular analysis of an auxin-binding protein gene located on chromosome 4 of *Arabidopsis*. Plant Cell 4: 193–201 (1992).
21. Rück A, Palme K, Venis MA, Napier RM, Felle RH: Patch-clamp analysis establishes a role for an auxin binding protein in the auxin stimulation of plasma membrane current in *Zea mays* protoplasts. Plant J 4: 41–46 (1993).
22. Sambrook J, Fritsch EF, Maniatis T: Molecular Cloning: A Laboratory Manual, 2nd ed. Cold Spring Harbor Laboratory Press, Cold Spring Harbor, NY (1989).
23. Schwob E, Choi SY, Simmons C, Migliaccio F, Ilag L, Hesse T, Palme K, Soll D: Molecular analysis of three maize 22 kDa auxin-binding protein genes: transient promoter expression and regulatory regions. Plant J 4: 423–432 (1993).
24. Shimomura S, Sotobayashi S, Futai M, Fukui T: Purification and properties of an auxin-binding protein from maize shoot membranes. J Biochem 99: 1513–1524 (1986).
25. Shimomura S: EMBL data library accession numbers X70902 and X70903 (1993).
26. Thiel G, Blatt MR, Fricker MD, White IR, Millner P: Modulation of K^+ channels in *Vicia* stomatal guard cells by peptide homologs to the auxin-binding protein C terminus. Proc Natl Acad Sci USA 90: 11493–11497 (1993).
27. Tillman U, Viola G, Kayser B, Siemester G, Hesse T, Palme K, Löbler M, Klämbt D: cDNA clones of the auxin-binding protein from corn coleoptiles (*Zea mays* L.): isolation and characterization by immunological methods. EMBO J 8: 2463–2467 (1989).
28. Venis MA, Napier RM: Auxin receptors and auxin binding proteins. Crit Rev Plant Sci 14: 27–47 (1995).
29. Venis MA, Napier RM, Barbier-Brygoo H, Maurel C, Perrot-Rechenmann C, Guern J: Antibodies to a peptide from the maize auxin-binding protein have auxin agonist activity. Proc Natl Acad Sci USA 89: 7208–7212 (1992).